NEWSLETTER
2020 / March

THESEUS FE

THESEUS-FE 8.0

- Manikin handling totally revised
- New Berkeley comfort models
- Improvement of contact algorithm
- Solar multi-band models
- New features for module OVEN
- New features for module E-COATING
- And many more …

ARRK

MANIKIN handling totally revised

In previous versions, a THESEUS-FE model consisted of a huge number of manikin keywords. Since version 8, the manikin definitions is much simpler. Basic properties like the metabolic activity are still defined using keyword MANIKIN. Just a handful of additional keywords are used to activate the thermal comfort indices (e.g. MANFPMV, MANFISO). Further manikin keywords are no longer needed. The new manikin keyword MANFINC (see figure 1) is used instead to compose the manikin model.

Four pre-defined manikin body models from literature are included in this release:

- Fiala neutral (based on D. Fiala's PhD thesis)
- European female (based on [1])
- European male (based on [1])
- Asian male (based on [2])

Our typical clothing ensembles are now available as manikin includes as well:

- Ensemble A (men's business suit)
- Ensemble B (men's summer casual)
- Ensemble C (jeans + shirt)
- Ensemble D (summer shorts + shirt)
- Ensemble E (business suit + winter jacket) and others

All these manikin include files can be found in the new version 8 installation folder in *#INST\Manikins*.

Radiation surface properties of garments are now stored together with the other physical properties of clothing (keyword MANFBCL). For this reason, the definition of radiation properties (keyword PRAD) is now obsolete on manikin surface.

	age	mass [kg]	height [m]	skin area [m²]	metabolism [W] at neutrality	body fat [%]
Fiala PhD	-	(73.5)	(1.71)	(1.86)	(87.1)	(14.4)
Fiala2 with modified abdomen	-	73.5	1.71	1.77	87.1	14.4
European female TFS	23	62.4 (61.5)	(1.69)	1.71 (1.70)	68.8 (69.2)	23.6 (23.9)
European male TMS	23	78.6 (78.3)	(1.81)	1.96 (1.96)	91.6 (91.8)	13.8 (13.7)
Asian male	30	64.9 (59.5)	(1.70)	1.70 (1.71)	66.4 (80.1)	15.5 (16.8)

Fig. 2: Manikins available in THESEUS-FE version 8 (values in brackets are reference values from literature)

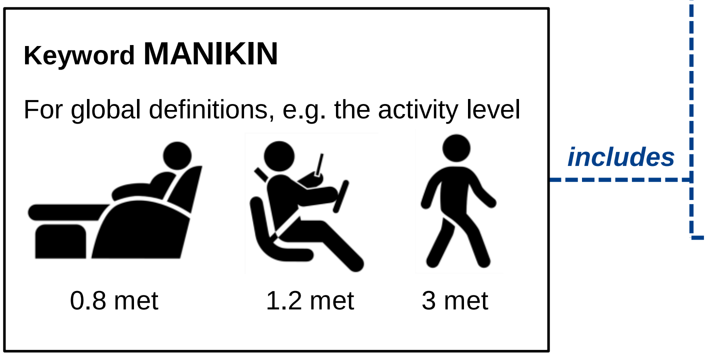

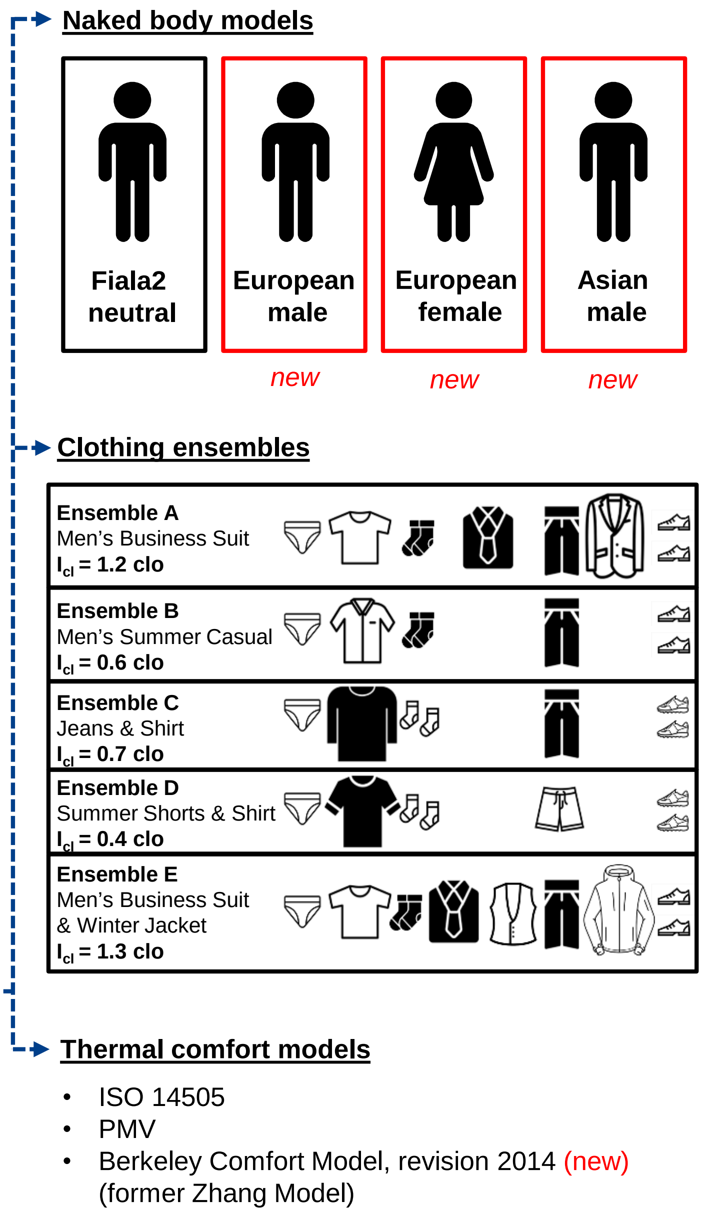

Fig. 1: New include structure of keyword MANIKIN

Figure 3 shows results from the validation suite for the Asian male manikin. We successfully compared simulation and test results from literature [2] with new results from THESEUS-FE. Details of the simulation and test are as follows:

- Environment temperature from 20°C to 34°C
- 1 h duration of experiments at T_{env}
- Relative humidity ~40%
- 15 healthy male Asian male subjects
- Sitting on chairs
- Activity level = 1 met
- I_{cl} = 0.6 clo (summer cloth)
- Low air speed (0.1 m/s)

Figure 3 also includes the results of mean skin temperature and rectal temperature in experiments and simulations. Results demonstrate a very good fit for Asian male. The blue curve shows higher skin temperatures for the neutral Fiala manikin for environment temperatures between 20°C and 28°C.

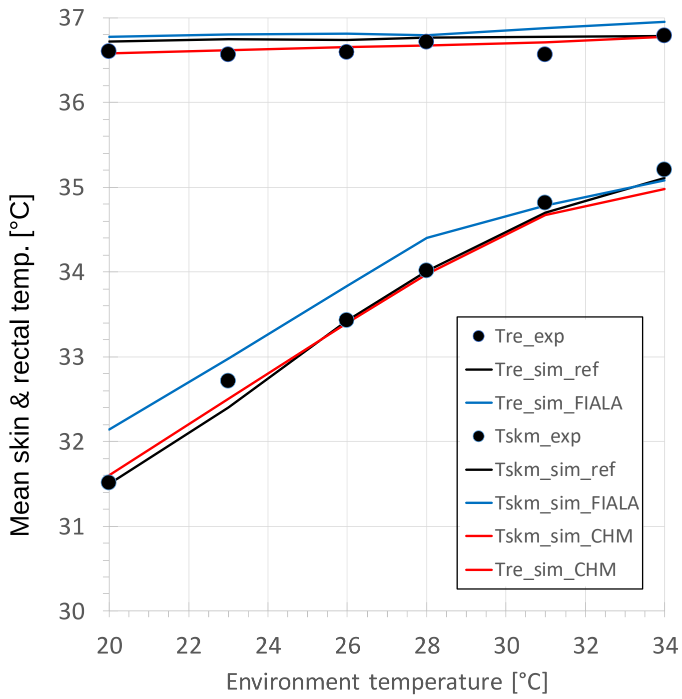

Fig. 3: Validation results for Asian male

The red curves in figure 4 show simulation results of the new female and male manikin models available in THESEUS-FE version 8 compared with experiments. As expected, the results show lower skin temperatures for the female manikin model in a cold environment (5°C). On some local body parts (e.g. arm) those differences in skin temperature can reach up to 4°C.

Whereas prior to version 8 it was cumbersome to change the manikin and clothing types, one can now easily switch from a male to female manikin by simply changing the manikin include file (keyword MANFINC). Clothing can be changed that easily as well.

Examples and validation cases are delivered with the installation of THESEUS-FE and are located at: *#INST\Examples\Validations\4_Fiala*

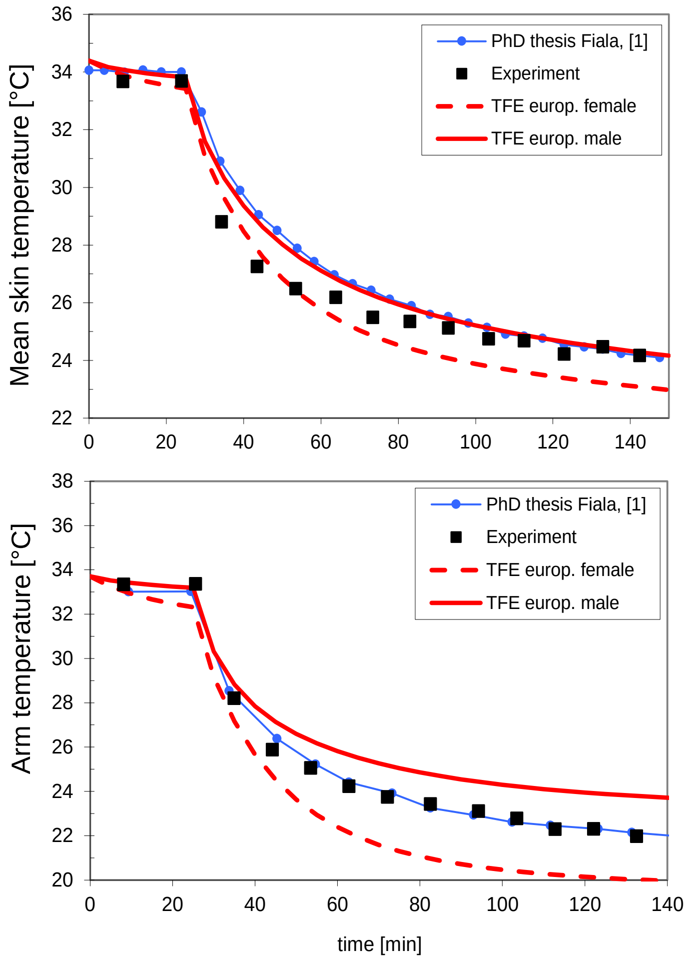

Fig. 4: Manikin validation at 5°C environmental temperature (ref.: Validation Manual, chapter 4.3.2)

New Berkeley comfort models

In 2010, Zhang et al. presented a series of papers ([3], [4], [5]) with modified sensation and comfort models. The models apply to sedentary activities in a range of uniform and non-uniform environments, stable and transient. Those models are based on literature review and on body-part-specific human subject tests in a climate chamber. They were validated against a test sample of automobile passengers.

The main changes concern the overall sensation model that has now two forms depending on whether all of the body parts have sensations effectively in the same direction (= "*no-opposite-sensation*") or some body parts have sensations opposite to those of the rest of the human body (= "*opposite-sensation*").

Based on these considerations, Zhang et al. have developed different models to derive the overall sensation index. To understand which model is used under what conditions, we have illustrated the underlying algorithm in figure 5a.

Regarding the opposite-sensation model, individual body parts now have different weights for warm versus cool sensations, and strong local sensations dominate the overall sensation. If all body part sensations remain near neutrality, the overall sensation is close to the average of the local sensations.

Time-dependent simulations showed that the transition from one overall sensation model to another could result in jumps in the curve. For that reason Zhao et al. presented an additional paper [6] in 2014 which helps to smooth the transition between these models (see fig. 6).

Starting with version 8.0 of THESEUS-FE it is highly recommended to use this latest model revision "2014" in the keyword MANFZLC as the thermal comfort model (see figure 5b).

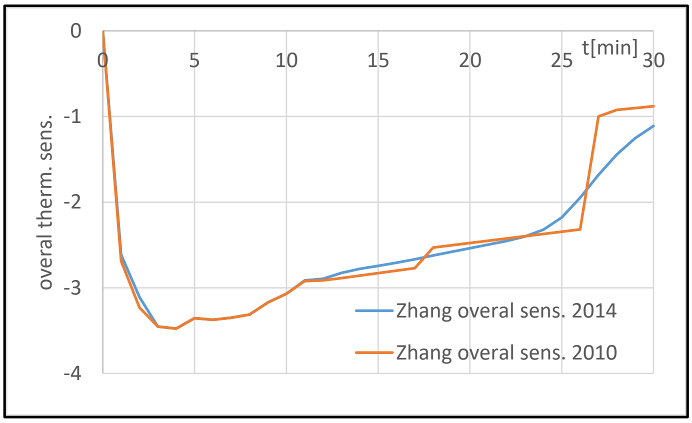

Fig. 6: Automotive winter load case example demonstrating the smoothing of Zhang's overall sensation from 2014

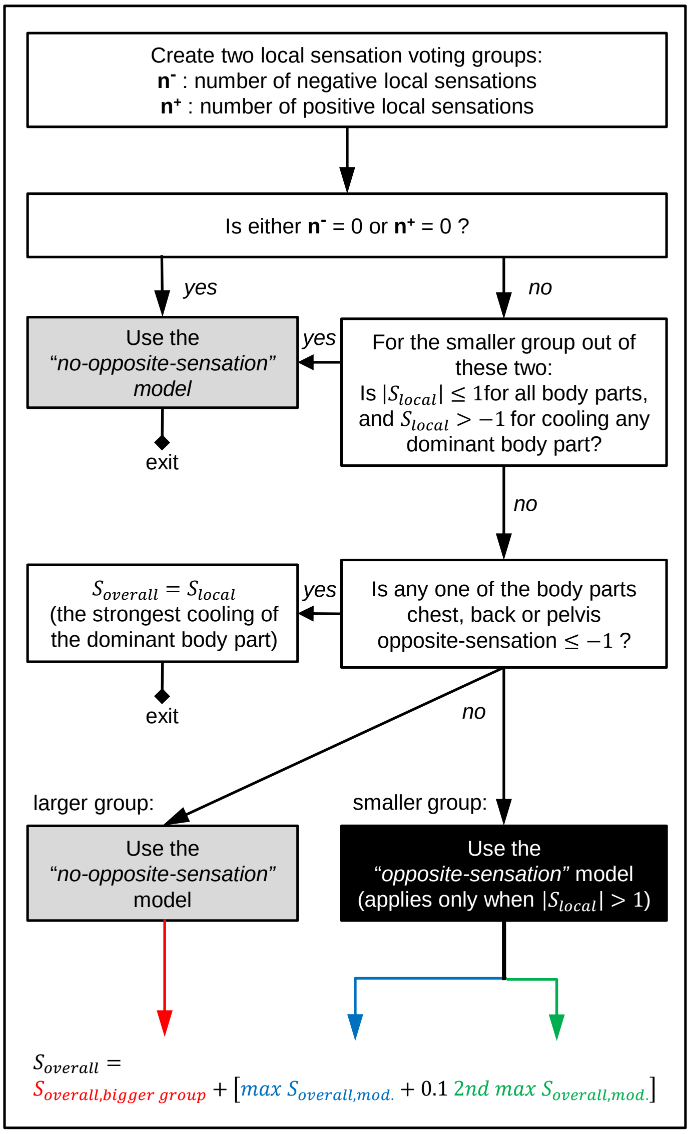

Fig. 5a: The new overall sensation algorithm

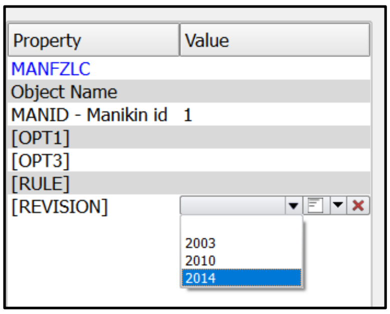

Fig. 5b: How to use the 2014 model

Paper [5] includes test results of thermal sensations that had been used to compare the old Zhang overall sensation model (from 2003) with the improved new one (see also figure 7). The subjects were exposed to uniform thermal conditions, but there are significant differences in local sensations of the body parts, because clothing and physiology are inherently non-uniform across the body. Overall sensation tends to be close to the most stressful (cold or hot) local sensations (= so-called "*complaint model*").

The red and blue boxes show

- coldest local sensations in cool environments at hands, arms, and feet
- warmest local sensations in warm environments at head, face and hands

See figures 7 and 8.

Test cases:	cold	slightly cool	slightly warm	hot
Numb. of tests:	5	6	3	10
Votes for local sens.:				
head	-1.4	-0.7	0.9	2.3
face	-1.4	-0.6	0.9	2.3
neck	-1.1	-0.6	0.8	1.9
chest	-2.2	-0.6	0.8	1.8
back	-1.6	-0.9	0.7	1.4
pelvis	-1.7	-0.6	0.5	1.3
arm	-3.3	-0.8	0.7	1.6
hand	-3.5	-0.6	0.7	1.9
leg	-2.6	-1.1	0.6	1.7
foot	-3.3	-1.7	0.5	0.8
Overall sensation:				
test	-3.1	-1.0	1.0	2.5
THESEUS-FE Zhang model 2003	-1.9	-1.0	0.7	1.8
THESEUS-FE Zhang model 2014	-3.4	-1.0	0.7	2.2

Fig. 7: Relations between local and overall sensations in test and simulation

For the two extreme test cases "cold" and "hot" the complete body distribution of the local sensation votes had been plotted with the THESEUS-FE graphical user interface (GUI) in figure 8.

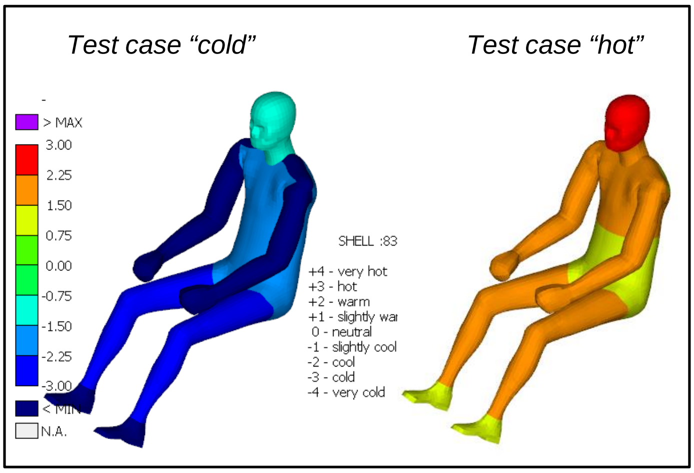

Fig. 8: Zhang local sensations in THESEUS-FE

In particular, for those two extreme test cases the overall sensation indices in figure 9 demonstrate the improved fit of the new Berkeley thermal comfort model compared with experiments.

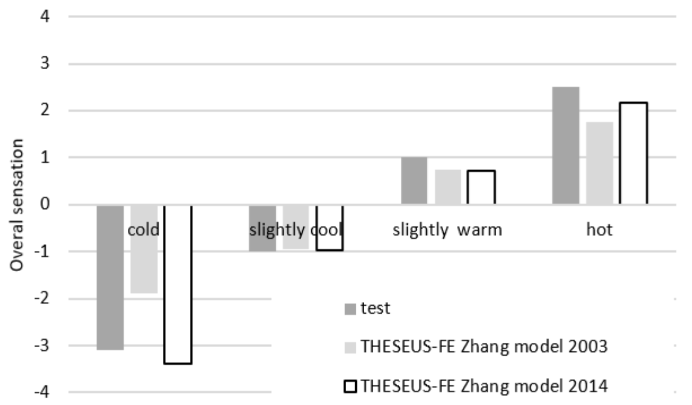

Fig. 9. Zhang overall sensation models vs. test

Zhang model 2014: new Berkeley thermal comfort model.

Complete revision of contact definitions

For the standard contact, the user defines for example the back of the manikin as the “master” and the surface of the seat as the “slave”. Since version 8, the definition of the minimum search distance (MIND) can now be omitted. Intersections will now always result in a contact irrespective of penetration distance.

Recommended settings for the standard manikin contact definitions are:

- General contact = No
- Search distance: MAXD = 0.01 m
- Shell thickness scale factor: STFS = 0

See figures 10

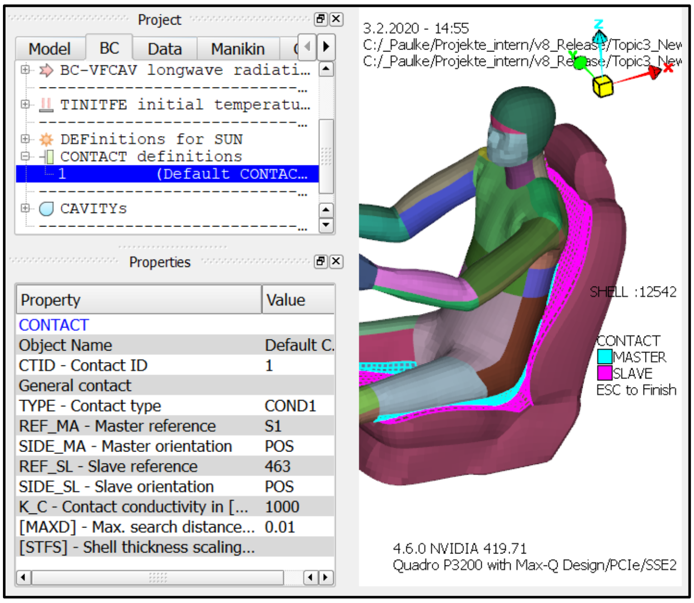

Fig. 10: Standard contact (pre-processing)

Any time using contact in a THESEUS-FE model, it is recommended plot the contact distance (master-slave) to better understand which elements are connected. See figure 11. To write out CTDST please define POSTDOF-CONTACT=YES. Negative values of the contact distance represent intersections.

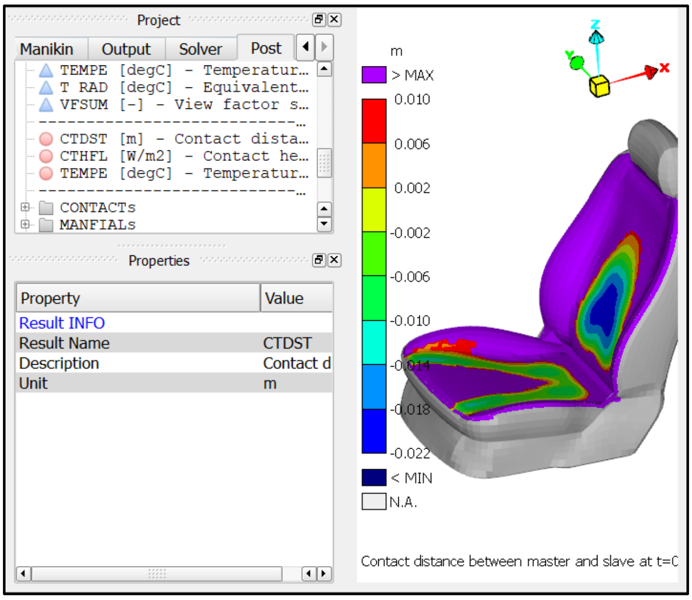

Fig. 11: Standard contact (post-processing)

Since typical shell models are generally meshed at the mid plane, a new parameter STFS (= shell thickness scale factor) has been introduced to subtract the real shell thickness of the contact partners at any position in the mesh. Please be aware that this is not appropriate for manikin contact. A typical application example for STFS is a THESEUS-FE Oven model with hundreds of metal parts with different sheet thicknesses.

See figure 12.

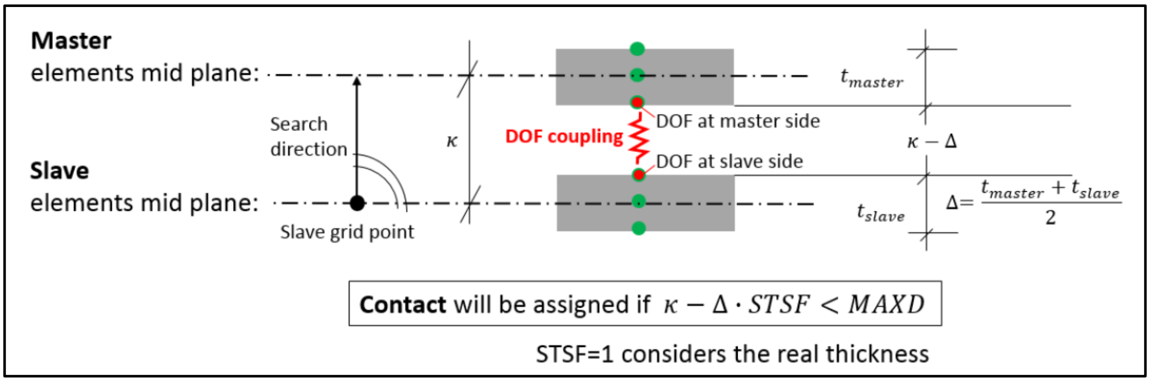

Fig. 12: The new contact algorithm

For non-manikin structures, it is much easier to apply a so called “General contact” where slave and master surface definitions are not required. Recommended settings for the general contact algorithm are:

- General contact = YES
- Search distance: MAXD = 0 m
- Shell thickness scale factor: STFS = 1-2

With these settings, all sheet metal structures of a complex Oven model can be automatically connected on both sides so that heat conduction takes place across different parts.

See figures 13 and 14.

In order to check the assigned contact distance in post-processing, it is recommended to output special field results using option CONTACT=YES in keyword POSTDOF. In order to display the contact areas between the sheets, it is now necessary to make the MAX color transparent:

- Choose MAX color *alpha channel* < 255 and
- Activate *global model transparency* (yellow arrow)

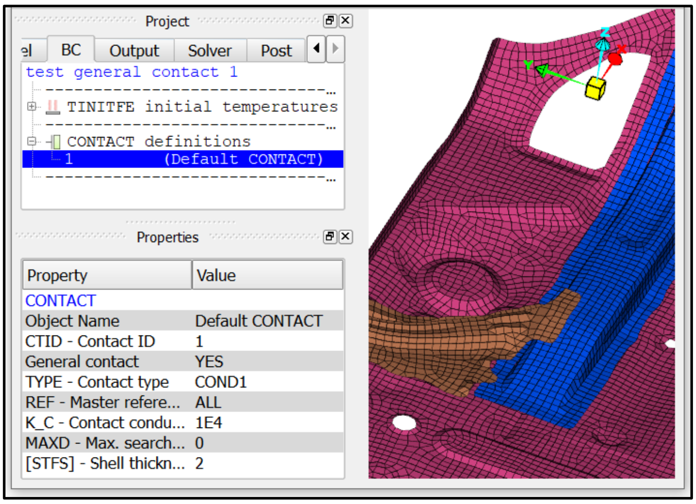

Fig. 13: General contact (pre-processing)

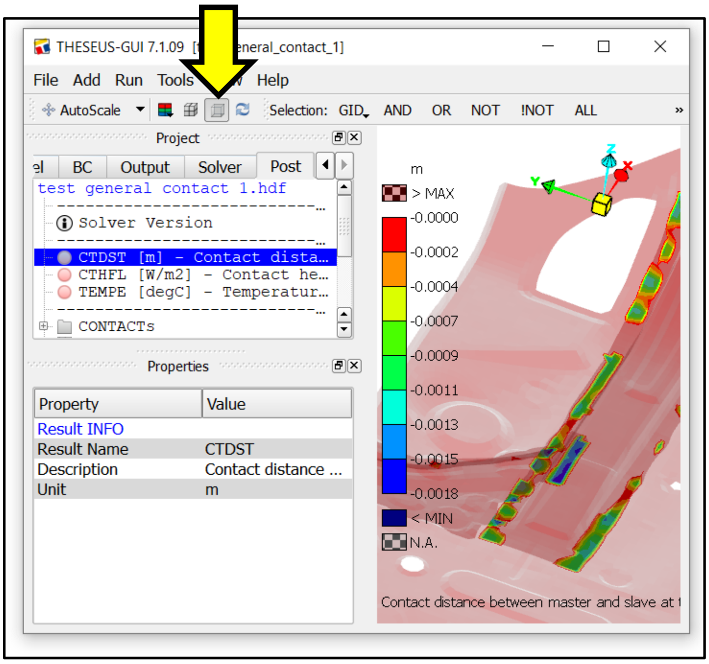

Fig. 14: General contact (post-processing)

Recommendation:
Due to the longer computing time, the contact algorithm should not be activated by default, but only if necessary or if the model does not contain connections weld spots and adhesives.

Solar multi-band models

Version 8 THESEUS-FE makes it possible to simulate multi-layered glass panes using wavelength-dependent properties for the refraction index, absorbance and solar intensities.

The key idea of this multi-band model is to define multiple sun objects using keyword DEFSUNS - one for each discrete wavelength quantity of interest. Each of these sun objects emits radiation waves of that specific wavelength. When these hit shell elements, the radiation properties for this specific wavelength are used.

To validate the new multi-band model we built a simple load case with two sun objects, two different wavelengths bands and four shell elements (representing the surfaces of the glass layers). See figure 15.

The radiation properties of the glass and the air layers are defined by the keyword PRADINT. Refraction index and absorbance are defined as functions of the wavelength as demonstrated in figure 16. The new keyword TABWVLN is used for defining those.

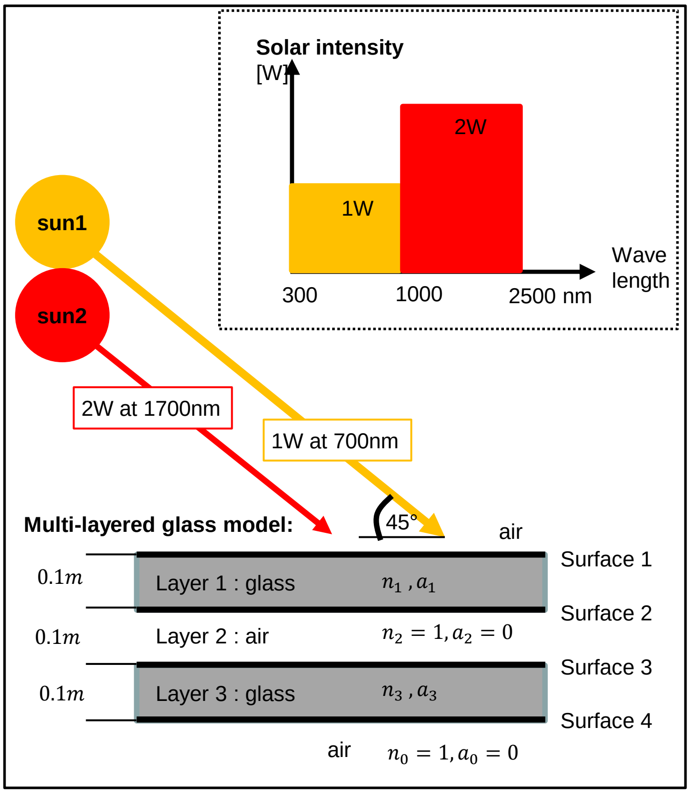

Fig. 15: Validation model for multi-band model

For multi-band models in THESEUS-FE there are various methods available for post-processing. You can

- check the path of each ray through each layer (see figure 16)
- check the totally transmitted and absorbed solar load on both sides of each layer

The system transmittance T, the system reflectance R and the system absorbance A have been validated with results from [7] chapter 18-2.
The THESEUS-FE solver applies the absorbed solar load as an internal heat source, which affects the temperature of the glass layer.

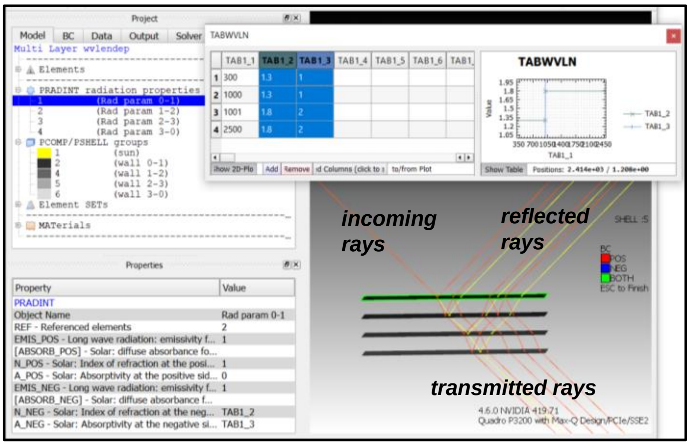

Fig. 16: Multi-band model in THESEUS-FE

Improvements for gap area calculation

In consultation with our customers, we recommend modifying some general parameters in the keyword OVEN to achieve a better fit for part temperatures inside larger cavities:

- Max. search dist. for gap temperature: DMX1 = 0.3
- Max. search dist. for gap heat transfer coefficient: DMX2 = 0.4

In this context, new field results can be plotted with the option POST_GAP=YES of the OVEN keyword:

The GAPFC field variable influences the heat transfer coefficient inside gaps and cavities:

$$h = h_{circ}(1 - GAPFC) + GAPFC \cdot h_{gap}$$

The GAPFT field variable influences the approximated air temperature inside gaps and cavities:

$$T_F = T_{circ}(1 - GAPFT) + GAPFT \cdot T_{gap}$$

The parameters DMX1 and DMX2 control the calculation of both gap factors (GAPFC, GAPFT).

New heat source type for OVENSEC

For the keyword OVENSEC a new heat source type “CAV” has been added.
It can be used to apply a predefined fluid temperature and a heat transfer coefficient to user-defined regions.
The region is specified using an element set. It can be further restricted to a single surface side and to areas where the gap temperature factor exceeds a certain threshold value. In the latter case only surfaces are considered where GAPFT ≥ MIN_GAPFT.
A typical application for an oven sector could be that hot air penetrates the sill through holes and an unknown air temperature arises inside. This air temperature could then be determined with the help of the calibration or directly tried to measure.

Heat source 6	CAV
[MIN_GAPFT] - 1st cavity condition, minimum GAPFC	0.6
T_C0 - Cavity air temperature in [°C]	25
H_CAV - Convective heat transfer coefficient on cavity facets in [W/(m2K)]	4
[SIDE] - 2nd cavity condition, element side	BOTH
REF - 3rd cavity condition, reference to element set	S3
[T_C_EXP] - Exponent in nonlinear formula for interpolating T_C	1
[T_C1] - Cavity air temperature at the end of the sector in [°C]	30
Heat source 7	CAV
[MIN_GAPFT] - 1st cavity condition, minimum GAPFC	
T_C0 - Cavity air temperature in [°C]	80
H_CAV - Convective heat transfer coefficient on cavity facets in [W/(m2K)]	20
[SIDE] - 2nd cavity condition, element side	POS
REF - 3rd cavity condition, reference to element set	S2

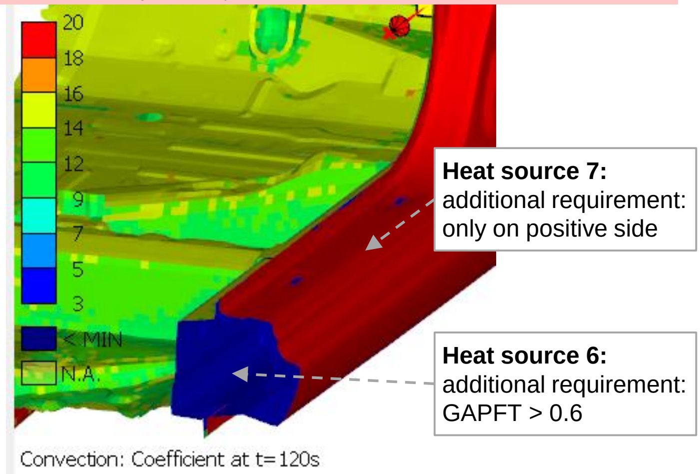

Fig 17: Example for the new OVENSEC heat source type “CAV”

New features for E-Coating Module

Version 7 introduced contact algorithms to insert holes into E-Coating structures. A good fit between coating results of models with holes geometrically represented in the solid mesh and models using contact definitions instead had been demonstrated.

Version 8 of THESEUS-FE adds a new tool called “Contact Assistant”. With this tool, holes can be added in E-Coating meshes very easily in a visually assisted manner. One can simply select a position in the shell mesh and choose the desired hole diameter (see figure 18).

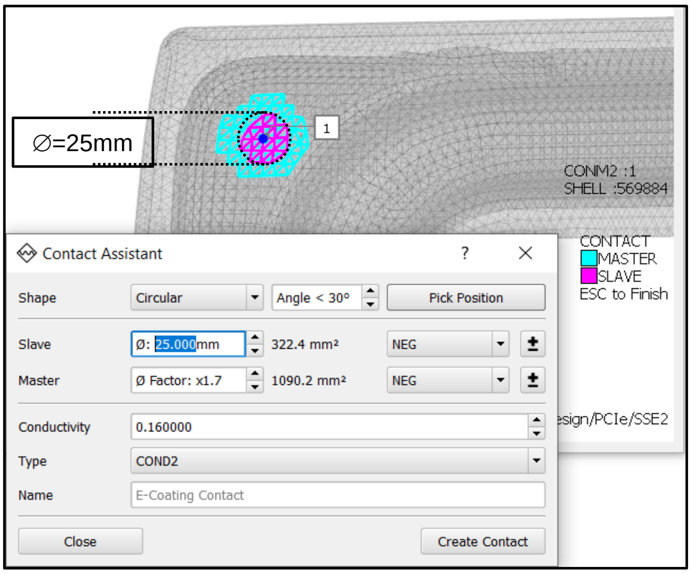

Fig 18: Contact Assistant

For a typical E-Coating calibration, the user defines single point mass elements at measurement positions and a global fit function with the POSTDAT keyword containing each measured paint thickness. After an automatic calibration, it is often helpful to visualize the difference between the measured and the simulated paint thickness at the measurement positions.
Version 8 includes the so-called “CONM2 Mapper” tool to greatly simplify this process (see figure 19).

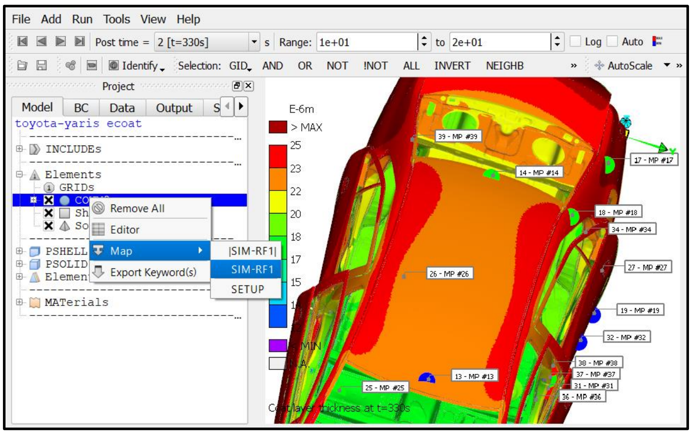

Fig 19: CONM2 Mapper

For example, the measuring points where the simulation deviates more than 2mm from the measurement can be represented as follows:

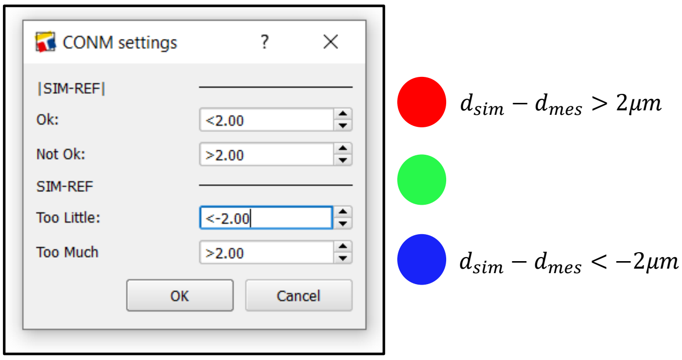

New ABAQUS Version Interfaces

Our Oven Module customers often use pre-calculated temperature fields from THESEUS-FE for thermally induced deformation analysis.
As new member of the Simulia partner program, THESEUS-FE provides interfaces to easily import and export data from and to ABAQUS for this purpose.

Import ABAQUS model file (.inp):
Read ABAQUS models originally created for structural mechanics (e.g. crash models).

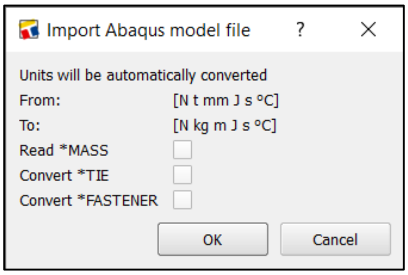

Export ABAQUS result file (.odb):
Write a binary ABAQUS result file, which contains mesh data and temperature field results at multiple time steps.

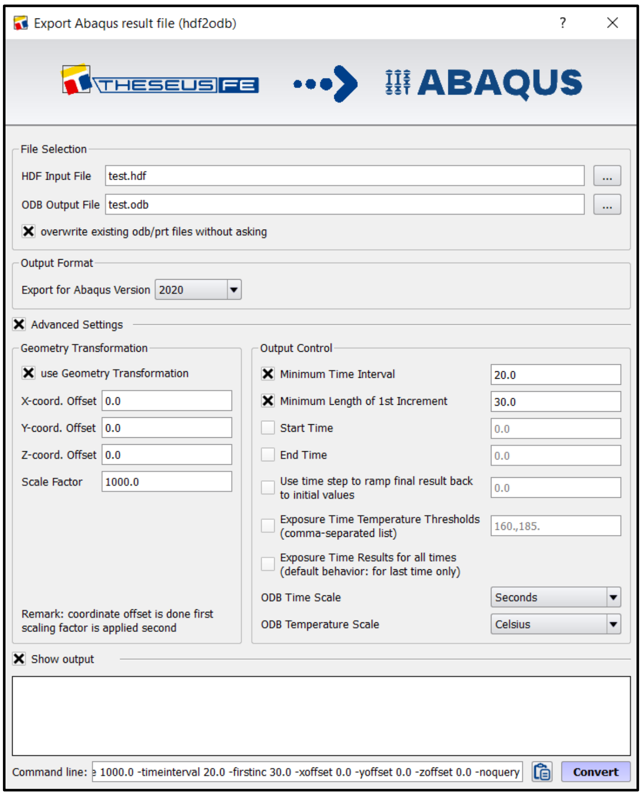

Temperature mapping can be done in ABAQUS or with our own mapping tool in the THESEUS-FE GUI.

Convenience features on Windows

The installer for Windows was fully revised for release 8. Additional information has been added so that Windows can display an extended version number and a file size estimate for the installation:

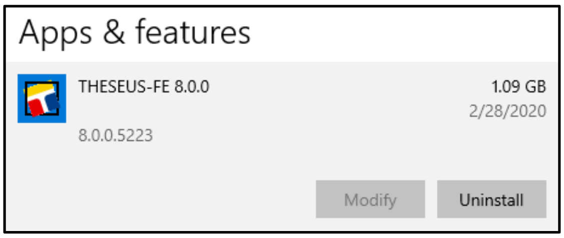

The uninstall process can now properly be run in unattended, silent mode.

Context menu entries can be added for Windows Explorer to conveniently open the THESEUS-FE GUI with the working directory set to the current directory and to quickly access the solver dialog:

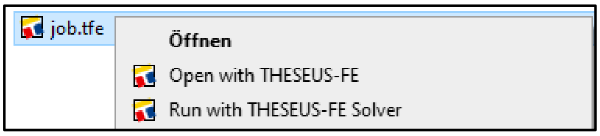

The THESEUS-FE documentation can now be accessed quickly directly from the GUI launcher:

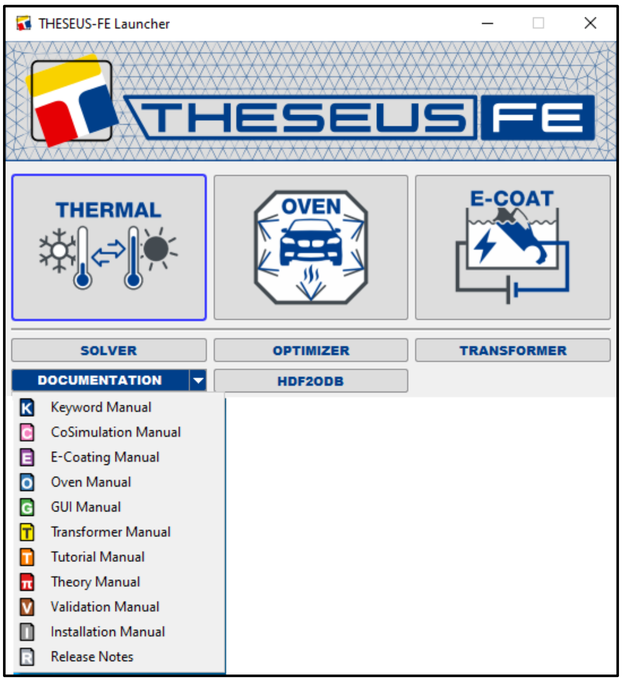

Upgrade of FlexNet Licensing

THESEUS-FE 8.0 uses the recent version 11.16.6.0 of FlexNet Publisher for licensing.
It will be necessary to upgrade existing installations of the license server “lmgrd”, maintenance tools like “lmutil” and our vendor daemon “puzld” to run this new version of THESEUS-FE.
Suitable versions of all programs are included in the installation packages and can be downloaded from our website separately as well.
Be sure to stop a running license server first, especially on Windows systems such that existing files can be overridden during the installation.

End-of-Support for some operating systems: Windows 7 and RHEL/CentOS 6

Windows 7 has already reached its official End-of-Life (EOL) date. Linux distributions Red Hat Enterprise Linux (RHEL) and CentOS 6 will soon reach theirs as well.
For that reason, THESEUS-FE 8.0 will not support these platforms.

THESEUS-FE 8.0 officially supports:

- Windows 10 (1709 and later)
- RHEL/CentOS 7 & 8

Bibliography

[1] Wölki Daniel: MORPHEUS: *Modelica-based implementation of a numerical human model involving individual human aspects*. PhD Thesis. Rwth Aachen (2017).

[2] Xin Zhou, Zhiwei Lian, Li Lan (2013): *An individualized human thermoregulation model for Chinese adults*. Building and Environments 70 (2013) 257-265.

[3] Hui Zhang, Edward Arens, Charlie Huizenga, Taeyoung Han: *Thermal sensation and comfort models for non-uniform and transient environments: Part I: Local sensation of individual body parts*. Building and Environment 45 (2010) 380–388.

[4] Hui Zhang, Edward Arens, Charlie Huizenga, Taeyoung Han: *Thermal sensation and comfort models for non-uniform and transient environments, part II: Local comfort of individual body parts*. Building and Environment 45 (2010) 389–398.

[5] Hui Zhang, Edward Arens, Charlie Huizenga, Taeyoung Han: *Thermal sensation and comfort models for non-uniform and transient environments, part III: Whole-body sensation and comfort*. Building and Environment 45 (2010) 399–410.

[6] Yin Zhao, Hui Zhang, Edward A. Arens, Qianchuan Zhao: *Thermal sensation and comfort models for non-uniform and transient environments, part IV: Adaptive neutral setpoints and smoothed whole-body sensation model.* Building and Environment 72 (2014) 300-308.

[7] Siegel R., Howell J.R: *Thermal Radiation Heat Transfer*. 4th Edition, 2002, Taylor & Francis

Imprint

Published approximately annually by P+Z Engineering GmbH, Munich, Germany.
For further information on P+Z Engineering GmbH please visit www.arrk-engineering.com

Editor: Dr. Stefan Paulke, stefan.paulke@arrk-engineering.com